

Manuscript version: Author's Accepted Manuscript

The version presented in WRAP is the author's accepted manuscript and may differ from the published version or Version of Record.

Persistent WRAP URL:

<http://wrap.warwick.ac.uk/106549>

How to cite:

Please refer to published version for the most recent bibliographic citation information. If a published version is known of, the repository item page linked to above, will contain details on accessing it.

Copyright and reuse:

The Warwick Research Archive Portal (WRAP) makes this work by researchers of the University of Warwick available open access under the following conditions.

Copyright © and all moral rights to the version of the paper presented here belong to the individual author(s) and/or other copyright owners. To the extent reasonable and practicable the material made available in WRAP has been checked for eligibility before being made available.

Copies of full items can be used for personal research or study, educational, or not-for-profit purposes without prior permission or charge. Provided that the authors, title and full bibliographic details are credited, a hyperlink and/or URL is given for the original metadata page and the content is not changed in any way.

Publisher's statement:

Please refer to the repository item page, publisher's statement section, for further information.

For more information, please contact the WRAP Team at: wrap@warwick.ac.uk.

Combining affinity selection and specific ion mobility for microchip protein sensing

William E. Arter,^{†,‡} Jérôme Charmet,^{‡,¶} Jinglin Kong,[†] Kadi L. Saar,[‡] Therese W. Herling,[‡] Thomas Müller,[§] Ulrich F. Keyser[†] and Tuomas P. J. Knowles^{†,‡,*}

[†]Cavendish Laboratory, University of Cambridge, JJ Thomson Avenue, Cambridge, CB3 0HE, UK

[‡]Department of Chemistry, University of Cambridge, Lensfield Road, Cambridge, CB2 1EW, UK

[¶]Institute of Digital Healthcare, International Digital Laboratory, WMG, University of Warwick, Coventry, CV4 7AL, UK

[§]Fluidic Analytics Ltd, Cambridge, UK

*Corresponding author. Email: tpjk2@cam.ac.uk

Abstract

The sensitive detection of proteins is a key objective in many areas of biomolecular science, ranging from biophysics to diagnostics. However, sensing in complex biological fluids is hindered by non-specific interactions with off-target species. Here, we describe and demonstrate an assay that utilises both the chemical and physical properties of the target species to achieve high selectivity, in a manner not possible by chemical complementarity alone, in complex media. We achieve this objective through a combinatorial strategy, by simultaneously exploiting free-flow electrophoresis for target selection, on the basis of electrophoretic mobility, and conventional affinity-based selection. In addition, we demonstrate amplification of the resultant signal by a catalytic DNA nano-circuit. This approach brings together the inherent solution-phase advantages of microfluidic sample handling with isothermal, enzyme-free signal amplification. With this method, no surface immobilisation or washing steps are required and our assay is well suited to mono-epitopic targets, presenting advantages over conventional ELISA techniques.

Introduction

The quantitation of target biomolecules in complex environments is essential in fundamental and applied protein science, including the development of novel diagnostics. In particular, proteins are an important class of biomarkers as they can be used to diagnose and monitor the activity of diseases and the efficacy of treatments.¹⁻³ Furthermore, compared to alternative biomarker species as investigated by transcriptional profiling⁴ and metabolomics,⁵ the protein domain is likely to be ubiquitously affected in disease, response and recovery.^{6,7} Therefore, developments in protein sensing are a promising route towards more accurate disease diagnostics and monitoring, with great potential in the emerging fields of point-of-care and personalised medicine.⁸

In contrast to nucleic acids, proteins cannot be amplified directly by PCR or other chemical biology techniques, and are subsequently challenging to detect when present at low concentrations against a complex background. Foremost amongst traditional analytic techniques is the enzyme-linked immunosorbent assay (ELISA), which typically relies on the surface-capture of a target by dual antibodies in a 'sandwich' complex, followed by enzyme-driven signal amplification. Whilst it remains the industry standard, ELISA is prone to false-positive signals due to non-specific surface-binding in complex assay media, and targets are usually required to be biepitopic.⁹⁻¹¹ Additionally, the use of perishable protein

1 reagents limits the application of ELISA for point-of-care applications in the field. Thus, sensing methods
2 that avoid surface-capture of targets, can be completed in a minimal number of steps and that employ
3 relatively more robust materials are of increasing interest.¹²⁻¹⁴

4 Here we propose an approach which combines electrophoretic, microfluidic separation and signal
5 amplification by DNA circuitry to enable the detection of proteins at biologically relevant, nM concentrations.
6 Physical specificity on the basis of electrophoretic mobility enables the quantitation of a target protein
7 against complex backgrounds including cell lysate medium. Our method avoids surface-capture of targets
8 and operates in an enzyme-free and isothermal manner. Though electrophoretic approaches have been
9 explored extensively in capillary-based end-labelled free-solution electrophoresis (ELFSE) for application in
10 DNA sequencing,¹⁵⁻¹⁸ protein-sensing methodologies and continuous sample fractionation based on similar
11 principles remain unexplored so far.

12 Microfluidic experiments permit efficient, fast and high-throughput analysis and enable the ready
13 manipulation and analysis of biomolecules based on their intrinsic physical properties. The application of an
14 electric field on chip permits electrophoretic analysis, with the response of analytes determined by both
15 hydrodynamic radii and net charge.¹⁹ Furthermore, as is common in bulk preparative and analytical
16 biochemistry assays, microfluidic electrophoresis also enables separation of biomolecular mixtures into
17 their constituent parts. For example, in microchip or capillary electrophoresis, molecules are separated *via*
18 differential migration along a microchannel under an electric field. However, typical capillary
19 electrophoresis-based methods are non-continuous, with analyses subsequently limited in throughput.²⁰⁻²²
20 The application of electric fields perpendicular to the direction of flow enables free-flow electrophoresis
21 (FFE), with experiments conducted in a continuous manner.²³⁻²⁷ Isoelectric focusing, a special case of FFE,
22 utilises this approach and can achieve excellent separation of biomolecules.^{26,28,29} Nonetheless, this
23 approach is complicated by the requirement of a suitable pH gradient, solution-phase stability of analyte
24 species at their isoelectric point (pI) and sufficient differences in pI between analytes for separation to be
25 successful. Therefore, FFE-based fractionation methods that utilise differences in analytes' electrophoretic
26 mobilities alone present several advantages, including the potential to operate in native, unperturbed
27 environments.

28 Following signal generation by isolation of the target species, signal amplification enables sensing of
29 targets present in low abundance. The rapidly growing field of DNA nanotechnology provides a means to
30 complement and improve upon protein-based signalling methods by providing DNA-based alternatives.
31 One area of interest is that of enzyme-free amplification *via* DNA-catalysed amplification circuitry, including
32 methodologies such as entropy-driven catalysis, hybridisation chain reaction and catalysed hairpin
33 assembly (CHA).³⁰⁻³³ These methods employ complementary 'toehold' base pairing of a target or signalling
34 nucleotide strand, in order to trigger binding between otherwise kinetically metastable DNA hairpins or
35 duplexes in a manner which enables linear, quadratic or exponential signal amplification. DNA circuitry is
36 inherently modular and scalable, has no requirement for degradable enzyme reagents and functions
37 isothermally, representing significant advantages over techniques such as polymerase chain reaction
38 (PCR), for example. Whilst DNA nanotechnology is increasingly being applied to biomolecular sensing,³⁰
39 attempts to link amplification schemes such as the CHA reaction with protein inputs have proved
40 challenging.³⁴

41 Our two-step approach allows for the selection of a single protein species against a complex
42 background, with simultaneous generation of a molecular signal that can be amplified through CHA. In the

development of this system, we have investigated the free-flow electrophoretic behaviour of a range of protein-appended ssDNA oligonucleotides, which show close agreement with previously published studies. This work represents an original approach to protein sensing, that can improve upon traditional methods where non-specific binding prevents accurate quantitation, for example when generic epitopes are shared between protein species.³⁵ Sensing experiments can be conducted on a shorter timescale (< 3.5 h) than is required by typical ELISA protocols, with no blocking or washing steps required. The target protein and capture species, streptavidin and biotin respectively, used for this model system were chosen so as to remove variability arising from protein binding kinetics. We demonstrate the working principle of the assay design with monovalent streptavidin as target, whilst work to develop this system for the sensing of protein targets of clinical interest is ongoing.

Methods

Microfluidic device fabrication

Devices were designed using AutoCAD software (Autodesk) and photolithographic masks printed on acetate transparencies (Micro Lithography Services). Polydimethylsiloxane (PDMS) devices were produced on SU-8 moulds fabricated *via* photolithographic processes as described elsewhere,^{36,37} with UV exposure performed with custom-built LED-based apparatus.³⁸ Following development of the moulds, feature heights were verified by profilometer (Dektak, Bruker) and PDMS (Dow Corning, primer and base mixed in 1:10 ratio) was applied and degassed before baking at 65 °C overnight. Devices were cut from the moulds and holes for tubing connection (0.75 mm) and electrode insertion (1.5 mm) created with biopsy punches, the devices were cleaned by application of Scotch tape and sonication in IPA (5 min). After oven drying, devices were bonded to glass slides using an oxygen plasma. Before use, devices were rendered hydrophilic *via* prolonged exposure to oxygen plasma.³⁹

Free-flow electrophoretic fractionation procedure

Flanking buffer solution (3750 µL/h, 0.1 X TE: 1 mM tris-HCl pH 7.5, 0.1 mM EDTA, 0.05% Tween-20), sample (40 µL/h, mixed in 0.1 X TE or cell lysate, supplemented with 0.05% Tween-20, 1% bovine serum albumin and 0.5% OliGreen® dye) and electrolyte (500 µL/h, 3M KCl, 1 µM fluorescein sodium salt) flow was controlled by syringe pumps (Cetoni neMESYS). Fluids were injected into the device *via* polythene tubing (Smiths Medical, 0.38 mm ID) from glass 1 mL or 0.5 mL syringes (0.5, 1 and 10 mL for sample, electrolyte and buffer, respectively; Hamilton). Potentials were applied by a benchtop power supply (Elektro-Automatik EA-PS 9500-06) *via* bent syringe tips inserted into the electrolyte outlets. Fractionated sample, flanking buffer and electrolyte was collected from tubing inserted into device outlets. Microfluidic experiments were observed and recorded on an inverted fluorescence microscope (Zeiss AxioObserver D1), fitted with appropriate filter cube and camera (Evolve 512 CCD, Photometrics). For each sample mixture, fractionated analyte was collected through continuous device operation over fifteen minutes.

Free-flow electrophoresis measurements

Data was gathered using devices containing integrated, solid electrodes in direct contact with the buffer stream in an analogous manner and using identical devices to that described previously.^{27,40}

Calibration of voltage efficiency

Voltage efficiencies for the electrophoretic devices were determined as described previously.⁴¹ Voltages were applied between 0-200 V with simultaneous measurement of the current between electrodes, for the device operating under experimental conditions and with the electrophoresis chamber filled with electrolyte. From the gradient of voltage plotted against current (three repeat measurements, see Supporting Information) electrical resistances of 800 k Ω and 450 k Ω were determined for the overall device and electrodes, respectively. The voltage resistance was determined by the relationship $(1 - \frac{\Omega_{electrode}}{\Omega_{device}})$ to afford a voltage efficiency of $\approx 44\%$.

Reagents and chemicals

ssDNA probes were imaged during microfluidic experiments *via* the addition of ssDNA-specific OliGreen[®] dye (200X stock dilution, Invitrogen) to samples. HPLC-purified DNA reagents were used as ordered from Integrated DNA Technologies, oligonucleotide base sequences are detailed in the Supporting Information. Monovalent streptavidin was procured from the laboratory of Mark Howarth, Oxford University,⁴² wild-type streptavidin was purchased from New England Biolabs. Streptavidin samples were incubated in TE buffer with biotinylated probe DNA in 1:4 molar ratio at room temperature for 20 minutes prior to experiment. Recombinant IgE (Bio-Rad) was buffer exchanged by spin column (Thermo-Scientific) into TGK buffer (192 mM glycine, 25 mM tris, 5 mM KH₂PO₄, pH 8.4) prior to aptamer probe binding by incubation at room temperature for fifteen minutes prior to experiment. Cell lysate was prepared from mouse 3T3 fibroblast cells ($\approx 1 \times 10^7$ / mL). Cells were centrifuged at 2000 rpm for five minutes and the supernatant removed. The cell pellet was then re-suspended in 1 mL 0.1 X TE buffer and washed a total of three times, before the cells were homogenised by passage through a 27G needle. The resulting lysate was passed through a 200 nm syringe filter and stored at 4 °C before further use.

Lyophilisation and CHA procedure

Samples collected from the electrophoresis step were supplemented with 1 μ M polyT₂₁ to prevent surface adsorption, flash-frozen and lyophilised. The resultant solids were re-dissolved in TNaK buffer (20 mM Tris (pH 7.5), 140 mM NaCl, 5 mM KCl) and transferred to a microwell plate (96-well half area, Corning) before CHA reaction. Immediately prior to CHA reaction, hairpins H1 and H2 were refolded by thermal annealing via heating at 90 °C for 1 minute, before cooling at a rate of 0.1 °C/s to room temperature. RepFQ reporter was prepared by thermal annealing of fluorescence reporter RepF and antisense quencher RepQ in 2:1 molar ratio. CHA reactions (70 μ L total volume) were conducted using a platereader (CLARIOstar, BMG Labtech) equipped with reagent auto-injector in TNaK buffer supplemented with 1 μ M pT₂₁ at 37 °C, with reagent concentrations of 400 nM H1, RepFQ and 1 μ M H2. Reaction mixtures equilibrated for 5 minutes prior to reaction initiation by auto-injection of H1 over a time period of <30 s.

Device operation for IgE sensing

In order to achieve effective separation of the IgE-aptamer probe complex from unbound aptamer probe, it was necessary to alter the ratio of fluidic resistance between the device outlets. A 50 cm length of tubing (0.305 mm ID) was inserted into the appropriate outlet (marked with *, Figure 1(b)) and raised to a height of 35 cm with a clamp stand. Alteration of the tubing height varies the pressure drop across the chip due to hydrostatic pressure, thus allowing easy adjustment of sample flow. The devices were operated at co-flow buffer, electrolyte and sample flow rates of 1100, 150 and 40 $\mu\text{L/h}$, respectively, with 100 V applied voltage.

Results and Discussion

Assay overview

Typically, conventional methods of protein sensing are founded upon affinity-based interaction of a surface-immobilised capture probe and target. Given the non-specificity associated with such methods, we sought to introduce an additional, orthogonal dimension for protein selection. Furthermore, we stipulated that throughout the assay protocol, our method should require no surface-immobilisation, washing steps or enzymatic reagents. To achieve these aims, we have developed a platform that combines the inherent solution-phase advantages of microfluidic sample handling, with specificity afforded by combined affinity and electrophoretic mobility-based selection. Moreover, signal is amplified isothermally and in an enzyme-free manner by DNA circuitry (Figure 1).

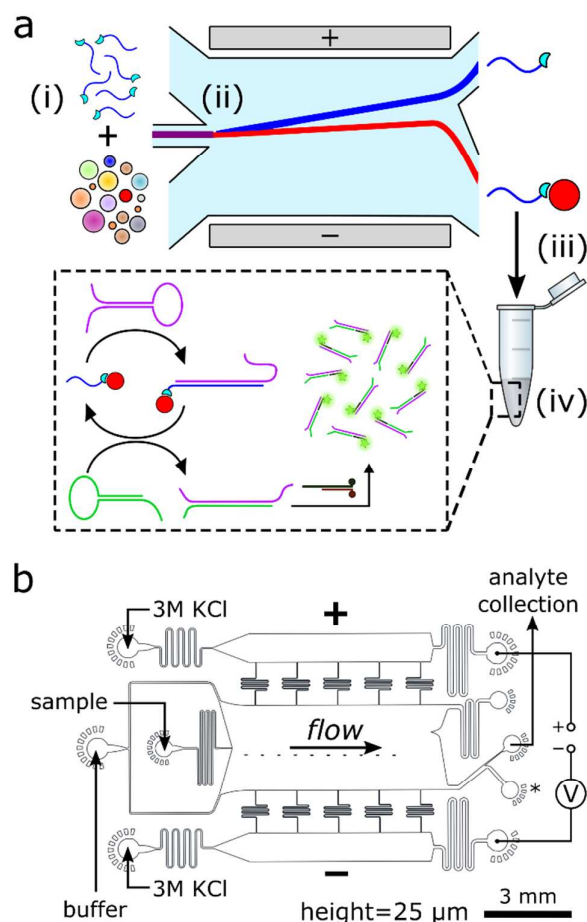


Figure 1. (a) Overview of the two-step assay. The target protein is shown in red. (i) Incubation of ssDNA probe strands with sample mixture. (ii) Free-flow electrophoretic separation of protein-bound and free

probe. (iii) Collection and re-concentration of isolated probe. (iv) Catalysed hairpin assembly assay with probe strand as catalyst for signal amplification and target quantitation. (b) Schematic of microfluidic device design and operation.

First, CHA-catalyst biotin-appended ssDNA probe oligos, with appropriate base sequence to enable their function as a CHA catalyst, are mixed in excess with the monovalent-streptavidin sample mixture (Figure 1(a.i)). Unbound probes are then separated from streptavidin-bound strands by continuous microfluidic free-flow electrophoresis (Figure 1(a.ii)). Off-chip, isolated strands are re-concentrated and CHA reaction is initiated (Figure 1(a.iii)), with the probe strands providing the catalyst for signal amplification and protein quantitation *via* fluorescence read-out (Figure 1(a.iv)).

Through our method, a molecular signal for CHA signal amplification from a single protein species is concurrently generated and isolated against a complex background. No surface-immobilisation or washing procedures are required, and the protein-orthogonal nature of signal amplification means that probe-protein recognition is only necessary in the electrophoretic fractionation step. Separation of the target species from the probe-sample mixture prevents false positives, and allows the use of high probe concentrations for effective target capture.

Electrophoretic fractionation of unbound probe from probe-protein complex

Biotinylated 25-nucleotide probe strands (see Supporting Information) were separated from the probe-monovalent streptavidin complex on chip using free flow electrophoresis. To enable the application of an electric field sufficient to effectively fractionate the probe required for subsequent CHA catalysis, a device design that makes use of liquid electrolyte electrodes was employed (Figure 1(b)). Voltages are applied *via* electrolyte (3M KCl + 1 μ M fluorescein) flowing through channels separate from the electrophoresis chamber, with field propagated into the device by the electrolyte.⁴¹ Fluorescein is added to the electrolyte solution to allow visualisation of the electrodes to aid device operation, whilst ssDNA was imaged by staining with a ssDNA-selective dye. The electrolyte flow flushes electrolysis products out of the chip, preventing flow instability, as well as reducing Joule heating of the device. With this system, separation of 25-base probe from its monovalent streptavidin complex was achieved (Figure 2).

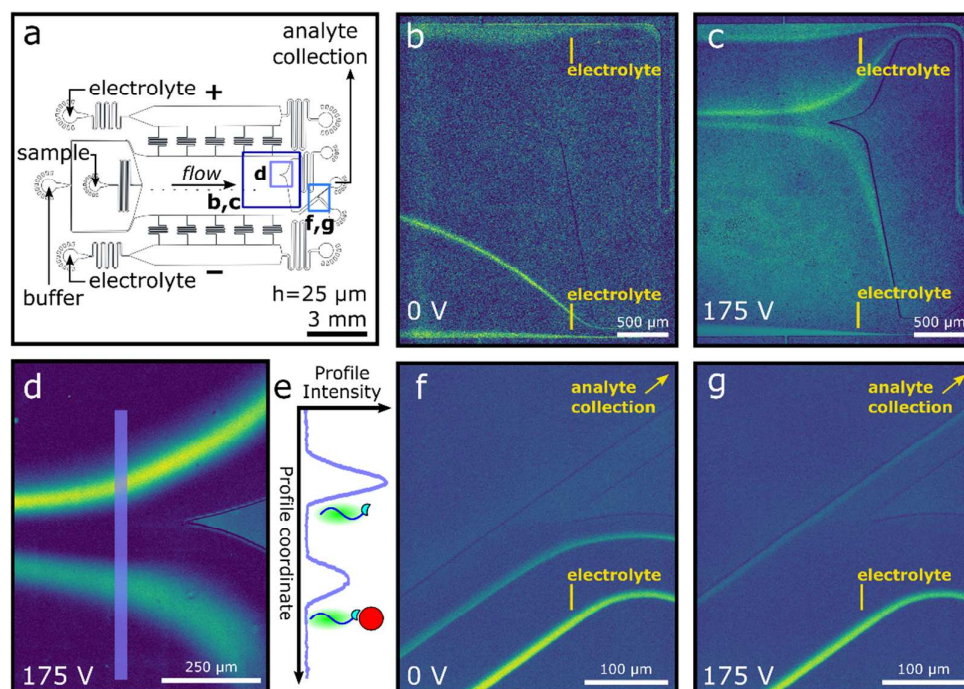


Figure 2. Physical selection of protein-probe target in free-flow electrophoresis device. Co-flow buffer, electrolyte (3M KCl + 1 μM fluorescein) and sample flow rates 3750, 500 and 40 $\mu\text{L/h}$, respectively. Species containing ssDNA were imaged by a ssDNA-selective stain (see Methods). (a) Schematic of overall device, denoting regions of interest shown in images. (b) Flow of analyte mixture with zero applied field, with electrode electrolyte observable at edges of channel. (c) Separation of 25-base probe from probe-monovalent streptavidin complex, with electrode electrolyte observable at edges of channel. (d) Magnified image of analyte fractionation, with intensity profile along purple line shown in (e). (f, g) Y-junction in device showing sample collection solely in the presence of the applied electric field and exclusion of electrolyte from collected fraction.

Buffer, electrolyte and sample were injected into the device by syringe pumps at flow rates of 3750, 500 and 40 $\mu\text{L/h}$ with a 175 V potential applied. Separation of the sample components was evidenced by the baseline fluorescence intensity observed between the sample streams (Figure 2(d)). Calibration of the device resistivity (see Methods) demonstrated a typical voltage efficiency of $\approx 40\%$, corresponding to an electric field of $\approx 230 \text{ Vcm}^{-1}$ at 175 V operating potential.

Selective isolation of the desired fraction was accomplished by the inclusion of a Y-junction in the sample exit channel (Figure 2(f, g)). With no voltage applied, the unfractionated probe/protein mixture, representing a false-positive signal, is not collected as the fluid flow directs the mixture into the waste channel. When the required voltage is applied, the fractionated analyte is electrophoretically diverted into the collection channel. Additionally, this feature ensures that the electrolyte mixture is excluded from the collected sample.

This feature imparts additional selectivity to the system, in addition to that afforded by probe-protein recognition. In the case where non-specific probe/target binding occurs, the resultant complex is unlikely to also possess the precise electrophoretic mobility required for collection and inclusion in the CHA assay. Therefore, our system, that relies on both the chemical and physical characteristics of the target species, may provide advantages in improving selectivity over non-specific or off-target probe-protein binding.

While the very strong biotin-streptavidin interaction represents a favourable case for the demonstration of this methodology in terms of probe/target binding kinetics, the successful separation of protein-aptamer complexes from the free aptamer using free-flow and capillary electrophoresis^{22,43} demonstrates that the application of this methodology to systems possessing weaker probe/target interactions should be possible with minor optimisation. Conversely, streptavidin represents a challenging target due to its negative charge. This hinders electrophoretic separation as the absolute value of the net charge of the probe-protein complex is higher than that for the free probe. Thus, separation on the basis of the probe-protein complex possessing a larger hydrodynamic radius relative to the free probe is offset to an extent by the probe-protein complex having a greater net charge. That separation is observed for streptavidin implies the suitability of this system for a generic protein target, with most proteins possessing a negative net charge at neutral pH.

Probe-catalysed hairpin assembly and signal amplification

Separation and selective collection of the probe-target complex enables accurate quantitation of the original protein sample, *via* amplification of the resultant probe signal by CHA reaction (Figure 3(a)).⁴⁴ During electrophoretic selection, the recovered target undergoes ≈ 16 -fold dilution on-chip. For the concentrations assayed here, subsequent quantitation by CHA reaction is possible directly from the recovered fraction. However, re-concentration of the fractionated sample by lyophilisation or speed-vacuum allows for simple normalisation of buffer conditions for the amplification step, and negates the decrease in assay sensitivity caused by on-chip dilution. Furthermore, this step provides the opportunity to increase assay sensitivity by recovering fractionated sample into the same CHA assay volume over a prolonged collection time. This process is made viable by the protein-orthogonal nature of the DNA circuitry, as the structure and function of the DNA probe is conserved in lyophilisation, in contrast to many protein analytes and reagents.

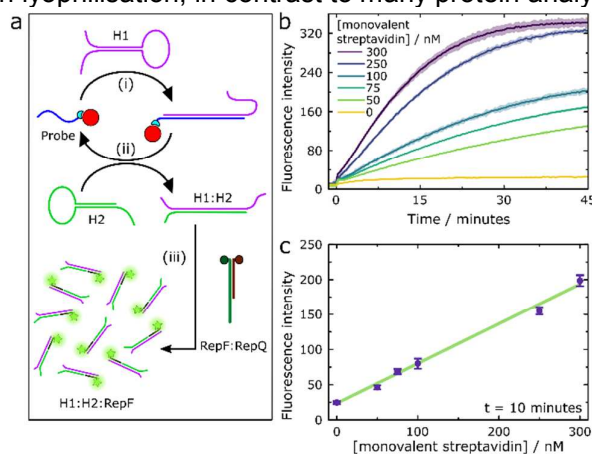


Figure 3. Target signal amplification and quantitation by catalysed hairpin assembly (CHA), following on-chip electrophoretic fractionation from probe/protein mixture. (a) Schematic showing the mechanism of the CHA reaction, catalysed by a probe-protein complex. (b) Signal amplification resulting from probe catalysis, with monovalent streptavidin present in original sample at concentrations ranging from 0-300 nM.

(c) Plot of CHA assay fluorescence intensity 10 min after circuit initiation as a function of initial target concentration, with a linear fit for monovalent streptavidin concentration between 0-300 nM. Error bars show standard deviation of three repeat measurements.

Following resuspension, hairpin H2 and quenched reporter RepFQ were added prior to reaction initiation by the addition of H1. Whilst they are ordinarily metastable, hybridization of H1 and H2 is catalysed by the probe *via* toehold-mediated strand displacement (Figure 3(a)). (i) First, the probe catalyst binds to the exposed 'toehold' domain of H1, enabling subsequent strand displacement of the intramolecularly-hybridized bases, resulting in opening of the hairpin. (ii) The newly exposed region of H1 acts as a toehold that is complementary to the single-stranded region of H2, this enables H1 and H2 to hybridize *via* strand displacement of the probe catalyst, which is then free to catalyse another cycle. (iii) Hybridisation of H1 and H2 exposes a single stranded region in H1 that is complementary to the toehold of the RepFQ reporter. The H1:H2 duplex hybridizes with RepF and displaces the quenching strand RepQ, resulting in signal turn-on.

CHA assays were performed on lyophilized analytes following electrophoretic fractionation of sample mixtures containing 0, 50, 75, 100, 250 and 300 nM monovalent streptavidin target (Figure 3(b)). A linear relationship between initial target concentration and fluorescence intensity was recorded 10 min after circuit initiation (Figure 3(c)), thus demonstrating the feasibility of protein sensing by the assay methodology presented here. Whilst we observe a small amount of signal for the 0 nM monovalent streptavidin control, this is consistent with inherent leakage of the CHA circuit due to some degree of synthetic impurity in the oligonucleotide reagents.⁴⁵ This result is supported by the observation of a similar amount of leakage with the circuit operated in isolation without catalyst oligomer (Supporting Information).

Whilst the sensing of biomolecules, and of nucleic acids in particular, *via* isothermal signal amplification has been of intense recent interest,⁴⁶⁻⁵⁰ few examples exist for the sensing of proteins *via* purely DNA-based enzyme-free methodologies. Many sensing schemes require polymerase, nicking enzymes or the incorporation of nanoparticle or bead-based approaches. For the purely nucleic acid-based methodologies that do exist, achieving acceptable signal:background in the generation of signal from a protein input is challenging.^{34,51} Therefore, this assay represents an original, isothermal, enzyme free method of protein sensing that uses solely DNA reagents in the amplification step. Furthermore, the modularity inherent in CHA sensing would enable ready adaptation of the detection method to alternative colorimetric or electrochemical outputs, for example.

Free-flow electrophoresis of protein-appended ssDNA oligonucleotides

For the system to demonstrate sensing accuracy without false-positive signal from unfractionated free probe, separation fidelity in the electrophoretic stage of the assay was required. To gain insight into the physical characteristics of the system, the electrophoretic mobilities of a variety of probe lengths and their protein complexes were investigated.

Free-flow electrophoretic analysis of biotinylated ssDNA oligos 15, 25 and 38 bases long and their monovalent and wild-type streptavidin complexes was conducted in a manner analogous to that reported previously (Figure 4).^{27,40} DNA was labelled by a ssDNA-specific stain added to the sample mixture, a description of the analysis protocol and representative data can be found in the Supporting Information.

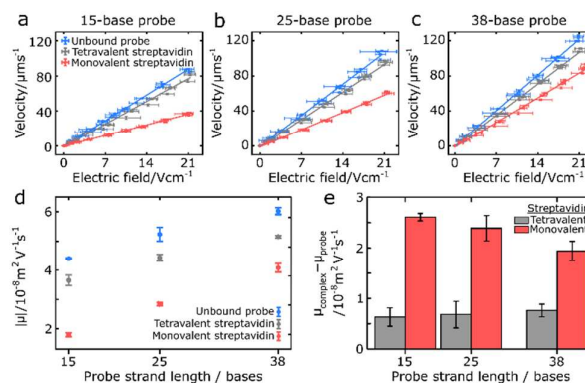


Figure 4. (a-c) Electrophoretic migration velocities perpendicular to fluid flow for biotinylated ssDNA probe strands and their complexes with monovalent and tetraivalent streptavidin for probe strands 15, 25 and 38 bases long, respectively. (d) Absolute values for the electrophoretic mobilities of biotinylated 15, 25 and 38-base ssDNA strands and their complexes with monovalent and tetraivalent streptavidin. (e) Difference in electrophoretic mobility (μ) between free probe and protein-bound probe complexes for 15, 25 and 38-base ssDNA. Error bars show standard deviation of three repeat measurements.

Notably, we observe that under these conditions unbound ssDNA strands do not behave as 'free-draining' polymers, in that their free-flow mobility is shown to increase with the length of the probe strand, in contrast to the behaviour predicted and reported by several previous studies.^{16,52,53} We ascribe this behaviour to the low salt (1 mM tris-HCl, 0.1 mM EDTA, pH 7.4) buffer used in these experiments. In this regime, intra-polymer hydrodynamic interactions are only poorly screened, resulting in size-dependent mobility.^{52,54,55} Furthermore, this behaviour was in close agreement to that predicted *via* theory⁵⁴ and determined experimentally under similar conditions *via* free-flow CE,⁵⁵ thus validating the continuous-flow microfluidic approach described here.

As demonstrated in the successful fractionation of monovalent streptavidin-probe complex from the unbound probe, monovalent and tetraivalent streptavidin-probe complexes were found to have reduced mobility relative to the unbound strand. In the case of the 1:1 monovalent streptavidin:probe complexes, the effect of the DNA-appended protein is to behave as a 'drag tag', thus reducing mobility relative to the free probe as described previously.^{18,56} This observation can be rationalised by considering the electrophoretic mobility $\mu = \frac{q}{6\pi\eta R_H}$, where q is the analyte charge, η the viscosity of the medium and R_H the hydrodynamic radius. Given the observed data, despite streptavidin being negatively charged at experimental pH, we infer that the increase in overall charge (q) that occurs with addition of the protein to the negatively charged DNA is insufficient to offset the concurrent increase in R_H , thus resulting in reduced mobility. Similarly, despite probes binding with 4:1 stoichiometry to tetraivalent streptavidin, the increase in complex charge is only enough to result in complex mobility intermediate to that of the unbound and monovalent streptavidin:probe complexes. As found computationally,¹⁸ for monovalent streptavidin $\Delta\mu = \mu_{\text{unbound}} - \mu_{\text{bound}}$ was shown to decrease with increasing strand length (4(e), Supporting Information (Table 1)).

In light of the mobility differences observed between the probe-protein complexes, we attempted to determine whether specific protein-probe complexes could be selectively isolated on an electrophoretic basis alone.

Enhanced specificity *via* electrophoretic selection

We have shown that electrophoretic fractionation provides a means to generate a protein signal, due to specific probe-protein binding resulting from chemical complementarity. Further to this, we demonstrate that the intrinsic differences in mobility between probe-protein complexes allows variable, physical selection of specific target species that would ordinarily remain indistinguishable by conventional host-guest selection alone (Figure 5).

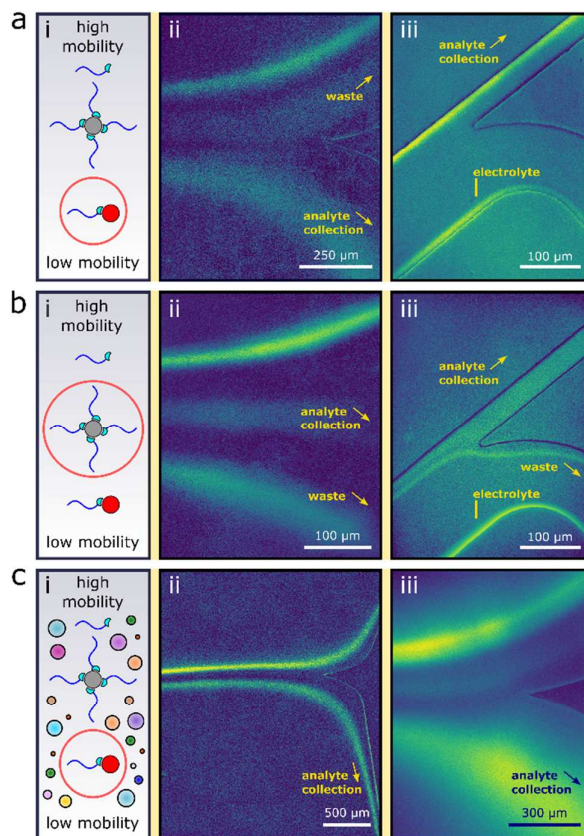


Figure 5. Variably selective isolation of specific probe-bound protein by electrophoretic mobility. (a(i)) Cartoon of selection of monovalent streptavidin-probe complex from tetraivalent streptavidin-probe complex and free probe on the basis of differential electrophoretic mobility. (a(ii)) Electrophoretic separation of monovalent streptavidin-probe target against tetraivalent streptavidin background and unbound probe. Tetraivalent streptavidin-probe complex is directed into the waste outlet. (a(iii)) Deflection of monovalent streptavidin-probe fraction into analyte collection channel. (b(i)) Cartoon of selection of tetraivalent streptavidin-probe complex from monovalent streptavidin-probe complex and free probe on the basis of differential electrophoretic mobility. (b(ii)) Electrophoretic separation of monovalent streptavidin-probe target against tetraivalent streptavidin background and unbound probe. (b(iii)) Deflection of tetraivalent streptavidin-probe fraction into analyte collection channel. Monovalent streptavidin-probe complex is directed into the waste outlet. (c(i)) Cartoon of selection of monovalent streptavidin-probe complex from tetraivalent streptavidin-probe complex and free probe in cell lysate. (c(ii)) Separation of monovalent streptavidin-probe complex from free probe in cell lysate. (c(iii)) Electrophoretic separation and selection of monovalent streptavidin-probe complex against tetraivalent streptavidin-probe complex background in cell lysate.

Using the same continuous free-flow electrophoresis methodology, probe-protein mixtures containing both monovalent and tetraivalent streptavidin were fractionated into their constituent parts, with relative mobilities concurrent with their determined values (Figure 5). Through manipulation of flow rate and

voltage, either the tetravalent or monovalent streptavidin-probe complex could be selectively isolated and collected (Figure 5(a) and (b), respectively). From probe-protein mixtures nominally containing 100, 200 and 300 nM monovalent and 30 nM tetravalent streptavidin, CHA amplification of the isolated monovalent-probe complex yielded measured concentrations of 97 ± 13 , 212 ± 35 and 319 ± 24 nM, respectively, by comparison to the linear fit determined previously (Figure 3(c)). An analogous experiment in the absence of monovalent streptavidin afforded only negligible CHA signal, confirming the effectiveness of signal isolation purely on the basis of electrophoretic mobility (Supporting Information).

Furthermore, the electrophoretic fractionation step was shown to be effective in a complex buffer environment. Monovalent streptavidin and probe were mixed in a solution of whole cell lysate ($\approx 1 \times 10^7$ cells / mL), before electrophoretic fractionation of the subsequent mixture on-chip (Figure 5(c.ii)). Despite the complex medium, the probe and probe-protein complex remained well fractionated, with fraction fluorescence intensities proportional to their respective concentrations added into the cell lysate mixture. From cell lysate mixtures containing probe and monovalent streptavidin at nominal concentrations of 300, 175, 100 and 50 nM, CHA amplification resulted in measured concentrations of 292 ± 13 , 167 ± 17 , 103 ± 11 and 42 ± 10 nM. Negligible CHA signal was observed in the absence of monovalent streptavidin, despite apparent fluorescence intensity in the analyte collection channel, which we attribute to non-specific interaction of the DNA-staining dye the cell lysate (Supporting Information). Furthermore, monovalent streptavidin could also be fractionated against tetravalent streptavidin background in the cell lysate (Figure 5(c.iii)), thus demonstrating the potential for the assay in real, complex samples.

Through the methodology presented here, chemical host-guest selectivity can be combined with and supplemented by physical, electrophoretic selectivity to enable the accurate sensing of species that would otherwise be limited by non-specific host-guest binding. Whilst both streptavidin proteins would be effectively recognised in the complex medium by generic biotin-binding alone, electrophoretic specificity is required to quantify the relative proportions of the two isomers. Together with the solution-phase, surface-free nature of the assay, this provides potential for improvement over traditional ELISA techniques, which can be limited by non-specific binding of analytes to capture antibodies or surfaces. Such approaches require laborious washing steps, and perturb the conformation of analyte and capture probes due to surface immobilisation.⁹⁻¹¹ Furthermore, strategies to minimise non-specific interactions such as sandwich-ELISA preclude their use for monoepitopic proteins, whereas the methodology presented here is valid for such targets. In our approach, non-specific sensing is avoided by the requirement for probe-bound species to possess a precise electrophoretic mobility required for analyte collection and signal generation, with the target protein reported in an entirely enzyme-free manner, and with an amplification system orthogonal to protein-binding chemistry.

Sensing of an antibody biomarker via aptamer probe

To demonstrate the applicability of the assay to a clinically relevant target, we adapted the system for the sensing of immunoglobulin E (IgE). IgE is a key component of the human immune system, with particular relevance in allergic response.⁵⁷ In addition, elevated IgE concentration is a defining characteristic of hyper IgE syndrome⁵⁸ and IgE myeloma,⁵⁹ making accurate quantitation of this biomarker an important diagnostic procedure.

Using an established anti-IgE DNA aptamer,⁶⁰ previous studies have shown free-flow electrophoretic separation of IgE-aptamer complex from unbound aptamer.⁶¹ Here, we expand on this approach by combining the aptamer sequence with that of the CHA catalyst to create a probe capable of both binding IgE and catalysing CHA reaction. A fluorophore was included at the terminus of the catalyst sequence to enable on-chip monitoring of the aptamer-probe behaviour. Due to the versatile nature of the microfluidic platform, only minor modification was necessary in order to optimise the assay for effective sensing of IgE (see Methods, Figure 6).

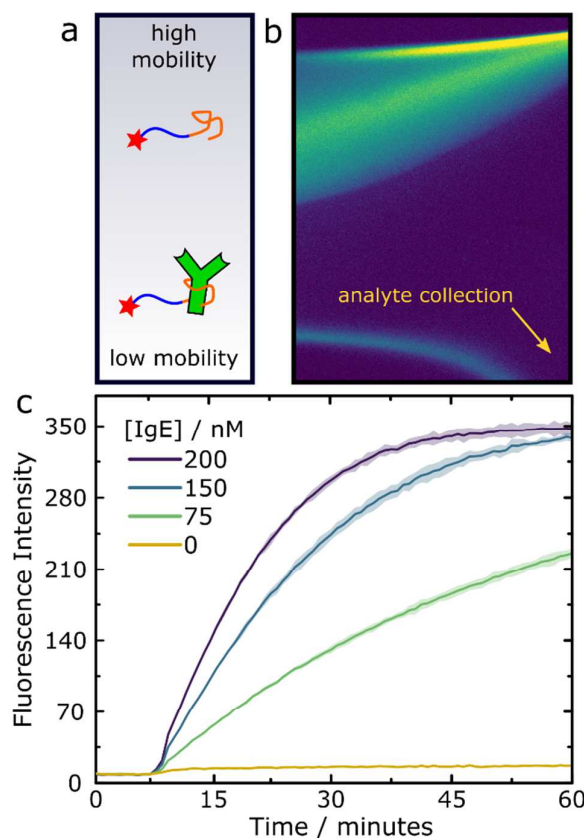


Figure 6. (a) Schematic of differential mobility between unbound aptamer probe and IgE-aptamer probe complex. The catalytic and aptameric sequences of the aptamer probe are represented by blue and orange sections, respectively. (b) Electrophoretic fractionation of IgE-aptamer probe complex from unbound probe. Flow rates 1100, 150, 40 $\mu\text{L}/\text{h}$ for co-flow buffer, electrolyte and sample, respectively. Applied voltage 100 V. (c) CHA signal amplification of isolated aptamer probe for initial IgE concentrations between 0-200 nM. Error bars represent standard deviation of three repeat experiments.

IgE-aptamer probe complex was electrophoretically isolated from unbound aptamer probe (Figure 6(b)), and the isolated probe was collected off-chip. The probe was then employed in CHA signal amplification by an analogous protocol to that described above (Figure 6(c)). Using this technique, a linear degree of amplification with respect to IgE concentration was observed (Supporting Information), with the aptamer probe added to the analyte solution at 4 μM concentration (at least 20-fold excess) to ensure complete binding of the IgE target.

The effective sensing of IgE by our assay demonstrates the modular nature of the proposed platform, which allows for the sensing of a wide range of protein targets simply by the introduction of a suitable aptamer. Indeed, our method provides advantages over conventional antibody-based oligonucleotide

detection methods such as immuno-PCR, as the bifunctional probe can be easily manufactured as a single oligo sequence, with oligo-antibody conjugation not required.

Conclusion

This paper describes a protein-sensing methodology combining chemical and physical selectivity. To this effect, the microfluidic FFE fractionation-based approach was shown to bypass selectivity limitations of conventional immunochemistry-based protein quantitation methods through the combination of chemical and physical selection criteria. In addition, the signal is amplified in an enzyme-free, isothermal manner via a nucleic-acid circuit in a catalysed hairpin assembly reaction, affording high sensitivity. We show that our assay performs effectively in complex biological environments, with target selectivity demonstrated in cell lysate. In future designs the CHA sensing step could be integrated into the same microfluidic platform as the electrophoretic step, enabling in-line, single-step and continuous sensing. With this assay, we have introduced an improved methodology for the detection of clinically relevant targets, as demonstrated by the sensing of IgE. Surface-free signal generation and the protein-orthogonal nature of the CHA amplification step is likely to be particularly advantageous in terms of assay specificity and simplicity in complex, physiological environments. Furthermore, apart from eliminating non-specific binding interactions, the integration of physical separation also allows multiple targets to be studied simultaneously even if they employ the same affinity probe. Additionally, multiple probes with orthogonal base sequences functionalised for different protein targets could enable multiplexed protein sensing via corresponding, orthogonal CHA circuits.

Supporting Information:

The following files are available free of charge. Figures S1-S5, numerical values for electrophoretic mobility data, DNA base sequences and modifications.

Supporting Information:

- Figures S1-S5
- Numerical values for electrophoretic mobility data
- DNA base sequences and modifications

Acknowledgement:

The research leading to these results has received funding from the European Research Council under the European Union's Seventh Framework Programme (FP7/2007-2013) through the ERC grant PhysProt (agreement 337969) and from the Newman foundation. W. E. A. acknowledges support from the EPSRC Cambridge NanoDTC, EP/L015978/1. K.L.S. acknowledges support from the EPSRC. T.W.H.

acknowledges support from the Oppenheimer Fund and the BBSRC. The authors thank the Howarth Lab,
University of Oxford for monovalent streptavidin samples.

1
2
3
4
5
6
7
8
9
10
11
12
13
14
15
16
17
18
19
20
21
22
23
24
25
26
27
28
29
30
31
32
33
34
35
36
37
38
39
40
41
42
43
44
45
46
47
48
49
50
51
52
53
54
55
56
57
58
59
60

References

1. Bateman, R. J.; Xiong, C.; Benzinger, T. L. S.; Fagan, A. M.; Goate, A.; Fox, N. C.; Marcus, D. S.; Cairns, N. J.; Xie, X.; Blazey, T. M.; Holtzman, D. M.; Santacruz, A.; Buckles, V.; Oliver, A.; Moulder, K.; Aisen, P. S.; Ghetti, B.; Klunk, W. E.; McDade, E.; Martins, R. N.; Masters, C. L.; Mayeux, R.; Ringman, J. M.; Rossor, M. N.; Schofield, P. R.; Sperling, R. A.; Salloway, S.; Morris, J. C. Clinical and Biomarker Changes in Dominantly Inherited Alzheimer's Disease. *N. Engl. J. Med.* **2012**, 367, 795–804.
2. Bui, M. H. T.; Seligson, D.; Han, K.; Pantuck, A. J.; Dorey, F. J.; Huang, Y.; Horvath, S.; Leibovich, B. C.; Chopra, S.; Liao, S.; Stanbridge, E.; Lerman, M. I. Palotie, A.; Figlin, R. A.; Beldegrun, A. S. Carbonic Anhydrase IX is an Independent Predictor of Survival in Advanced Renal Clear Cell Carcinoma : Implications for Prognosis and Therapy. *Clin. Cancer Res.* **2003**, 9, 802–811.
3. Rubin, M. A.; Zhou, M.; Dhanasekaran, S. M.; Varambally, S.; Barrette, T. R.; Sanda, M. G.; Pienta, K. J.; Ghosh, D.; Chinnaiyan, A. M. α -Methylacyl Coenzyme A Racemase as a Tissue Biomarker for Prostate Cancer. *JAMA* **2002**, 287, 1662–1670.
4. Ramaswamy, S.; Perou, C. M. DNA Microarrays in Breast Cancer: the Promise of Personalised Medicine. *Lancet* **2003**, 361, 1576–1577.
5. Fernie, A. R.; Trethewey, R. N.; Krotzky, A. J.; Willmitzer, L. Innovation: Metabolite Profiling: From Diagnostics to Systems Biology. *Nat. Rev. Mol. Cell Biol.* **2004**, 5, 763–769.
6. Rifai, N.; Gillette, M. A.; Carr, S. A. Protein Biomarker Discovery and Validation: the Long and Uncertain Path to Clinical Utility. *Nat. Biotechnol.* **2006**, 24, 971–983.
7. Eisele, Y. S.; Monteiro, C.; Fearn, C.; Encalada, S. E.; Wiseman, R. L.; Powers, E. T.; Kelly, J. W. Targeting Protein Aggregation for the Treatment of Degenerative Diseases. *Nat. Rev. Drug Discov.* **2015**, 14, 759–780.
8. Ahmed, M. U.; Saaem, I.; Wu, P. C.; Brown, A. S. Personalized Diagnostics and Biosensors: a Review of the Biology and Technology Needed for Personalized Medicine. *Crit. Rev. Biotechnol.* **2014**, 34, 180–196.
9. Güven, E.; Duus, K.; Lydolph, M. C.; Svaerke Jørgensen, C.; Laursen, I.; Houen, G. Non-Specific Binding in Solid Phase Immunoassays for Autoantibodies Correlates with Inflammation Markers. *J. Immunol. Methods* **2014**, 403, 26–36.
10. Gibbs, J. Effective Blocking Procedures ELISA Technical Bulletin - No 3, Corning Inc., Life Sciences. **2001**
11. Xiao, Y.; Isaacs, S. N. Enzyme-Linked Immunosorbent Assay (ELISA) and Blocking with Bovine Serum Albumin (BSA) - Not All BSAs Are Alike. *J. Immunol. Methods* **2012**, 384, 148–151.
12. Lin, X.; Sun, X.; Luo, S.; Liu, B.; Yang, C. Development of DNA-Based Signal Amplification and Microfluidic Technology for Protein Assay: a Review. *Trends Anal. Chem.* **2016**, 80, 132–148.
13. Tang, M. Y. H.; Shum, H. C. One-step Immunoassay of C-reactive Protein Using Droplet Microfluidics. *Lab Chip* **2016**, 16, 4359–4365.
14. Shim, J. U.; Ranasinghe, R. T.; Smith, C. A.; Ibrahim, S. M.; Hollfelder, F.; Huck, W. T. S.; Klenerman, D.; Abell, C. Ultrarapid Generation of Femtoliter Microfluidic Droplets for Single-Molecule-Counting Immunoassays. *ACS Nano* **2013**, 7, 5955–5964.
15. Fahrenkopf, M. A.; Mukherjee, T.; Ydstie, B. E.; Schneider, J. W. Optimization of ELFSE DNA Sequencing with EOF Counterflow and Microfluidics. *Electrophoresis* **2015**, 35, 3408–3414.
16. Mayer, P.; Slater, G. W.; Drouin, G. Theory of DNA Sequencing Using Free-Solution Electrophoresis of Protein-DNA Complexes. *Anal. Chem.* **1994**, 66, 1777–1780.
17. Meagher, R. J.; Won, J.-I.; McCormick, L. C.; Nedelcu, S.; Bertrand, M. M.; Bertram, J. L.; Drouin, G.; Barron, A. E.; Slater, G. W. End-Labeled Free-Solution Electrophoresis of DNA. *Electrophoresis* **2005**, 26, 331–350.
18. Grass, K.; Holm, C.; Slater, G. W. Optimizing End-Labeled Free-Solution Electrophoresis by Increasing the Hydrodynamic Friction of the Drag Tag. *Macromolecules* **2009**, 42, 5352–5359.
19. Beebe, D. J.; Mensing, G. A.; Walker, G. M. Physics and Applications of Microfluidics

- in Biology. *Annu. Rev. Biomed. Eng.* **2002**, 4, 261–286.
20. Chen, L.; Ren, J. High-Throughput DNA Analysis by Microchip Electrophoresis. *Comb. Chem. High Throughput Screen.* **2004**, 7, 29–43.
21. Hall, G. H.; Glerum, M. D.; Backhouse, C. J. A Light Emitting Diode, Photodiode-Based Fluorescence Detection System for DNA Analysis with Microchip Electrophoresis. *Electrophoresis* **2016**, 37, 406–413.
22. Lin, X.; Chen, Q.; Liu, W.; Yi, L.; Li, H.; Wang, Z.; Lin, J. M. Assay of Multiplex Proteins from Cell Metabolism Based on Tunable Aptamer and Microchip Electrophoresis. *Biosens. Bioelectron.* **2015**, 63, 105–111.
23. Raymond, D. E.; Manz, A.; Widmer, H. M. Continuous Sample Pretreatment Using a Free-Flow Electrophoresis Device Integrated onto a Silicon Chip. *Anal. Chem.* **1994**, 66, 2858–2865.
24. Fonslow, B. R.; Bowser, M. T. Free-Flow Electrophoresis on an Anodic Bonded Glass Microchip. *Anal. Chem.* **2005**, 77, 5706–5710.
25. Kohlheyer, D.; Eijkel, J. C.; van den Berg, A.; Schasfoort, R. B. Miniaturizing Free-Flow Electrophoresis - A Critical Review. *Electrophoresis* **2008**, 29, 977–993.
26. Turgeon, R. T.; Bowser, M. T. Micro Free-Flow Electrophoresis: Theory and Applications. *Anal. Bioanal. Chem.* **2009**, 394, 187–198.
27. Herling, T. W.; Müller, T.; Rajah, L.; Skepper, J. N.; Vendruscolo, M.; Knowles, T. P. J. Integration and Characterization of Solid Wall Electrodes in Microfluidic Devices Fabricated in a Single Photolithography Step. *Appl. Phys. Lett.* **2013**, 102, 184102.
28. Lu, H.; Gaudet, S.; Schmidt, M. A.; Jensen, K. F. A Microfabricated Device for Subcellular Organelle Sorting. *Anal. Chem.* **2004**, 76, 5705–5712.
29. Hosken, B. D.; Li, C.; Mullappally, B.; Co, C.; Zhang, B. Isolation and Characterization of Monoclonal Antibody Charge Variants by Free Flow Isoelectric Focusing. *Anal. Chem.* **2016**, 88, 5662–5669.
30. Jung, C.; Ellington, A. D. Diagnostic Applications of Nucleic Acid Circuits. *Acc. Chem. Res.* **2014**, 47, 1825–1835.
31. Zhang, D. Y.; Turberfield, A. J.; Yurke, B.; Winfree, E. Engineering Entropy-Driven Reactions and Networks Catalyzed by DNA. *Science* **2007**, 318, 1121–1125.
32. Yin, P.; Choi, H. M. T.; Calvert, C. R.; Pierce, N. A. Programming Biomolecular Self-Assembly Pathways. *Nature* **2008**, 451, 318–322.
33. Dirks, R. M.; Pierce, N. A. Triggered Amplification by Hybridization Chain Reaction. *PNAS* **2004**, 101, 15275–15278.
34. Du, Y.; Zhen, S. J.; Li, B.; Byrom, M.; Jiang, Y. S.; Ellington, A. D. Engineering Signaling Aptamers That Rely on Kinetic Rather Than Equilibrium Competition. *Anal. Chem.* **2016**, 88, 2250–2257.
35. Greiner, E. R.; Kelly, J. W.; Palhano, F. L. Immunoprecipitation of Amyloid Fibrils by the Use of an Antibody that Recognizes a Generic Epitope Common to Amyloid Fibrils. *PLoS ONE* **2014**, 9, e105433.
36. Mazutis, L.; Gilbert, J.; Ung, W. L.; Weitz, D. A.; Griffiths, A. D.; Heyman, J. A. Single-Cell Analysis and Sorting Using Droplet-Based Microfluidics. *Nat. Protocols* **2013**, 8, 870–891.
37. McDonald, J. C.; Duffy, D. C.; Anderson, J. R.; Chiu, D. T.; Wu, H.; Schueller, O. J. A.; Whitesides, G. M. Fabrication of Microfluidic Systems in Poly(dimethylsiloxane). *Electrophoresis* **2000**, 21, 27–40.
38. Challa, P. K.; Kartanas, T.; Charmet, J.; Knowles, T. P. J. Microfluidic Devices Fabricated Using Fast Wafer-Scale LED-Lithography Patterning. *Biomicrofluidics* **2017**, 11, 014113.
39. Tan, S. H.; Nguyen, N.-T.; Chua, Y. C.; Kang, T. G. Oxygen Plasma Treatment for Reducing Hydrophobicity of a Sealed Polydimethylsiloxane Microchannel. *Biomicrofluidics* **2010**, 4, 32204.
40. Herling, T. W.; Arosio, P.; Müller, T.; Linse, S.; Knowles, T. P. J. A Microfluidic Platform for Quantitative Measurements of Effective Protein Charges and Single Ion Binding in Solution. *Phys. Chem. Chem. Phys.* **2015**, 17, 12161–12167.
41. Saar, K. L.; Zhang, Y.; Muller, T.; Challa, P. K.; Devenish, S.; Andrew, L.; Knowles, T. P. J. On Chip Label Free Protein Analysis with Downstream Electrodes for Direct Removal of Electrolysis Products. *Lab Chip* **2018**, 18, 162–170.
42. Howarth, M.; Chinnapen, D. J.-F.; Gerrow, K.; Dorrestein, P. C.; Grandy, M. R.; Kelleher, N. L.; El-Husseini, A.; Ting, A. Y. A Monovalent Streptavidin With a Single Femtomolar

Biotin Binding Site. *Nat. Methods* **2006**, 3, 267–273.

43. Jing, M.; Bowser, M. T. Isolation of DNA Aptamers Using Micro Free Flow Electrophoresis. *Lab Chip* **2011**, 11, 3703–3709.

44. Li, B.; Ellington, A. D.; Chen, X. Rational, Modular Adaptation of Enzyme-Free DNA Circuits to Multiple Detection Methods. *Nucleic Acids Res.* **2011**, 39, e110.

45. Chen, X.; Briggs, N.; McLain, J. R.; Ellington, A. D. Stacking Nonenzymatic Circuits for High Signal Gain. *PNAS* **2013**, 110, 5386–91.

46. Spoto, G. Integration of Isothermal Amplification Methods in Microfluidic Devices : Recent Advances. *Biosens. Bioelectron.* **2017**, 90, 174–186.

47. Choi, H. M. T.; Beck, V. A.; Pierce, N. A. Next-Generation in situ Hybridization Chain Reaction: Higher Gain, Lower Cost, Greater Durability. *ACS Nano* **2014**, 8, 4284–4294.

48. Zhou, X.; Liang, Y.; Xu, Y.; Lin, X.; Chen, J.; Ma, Y.; Zhang, L.; Chen, D.; Song, F.; Dai, Z.; Zou, X. Triple Cascade Reactions: An Ultrasensitive and Specific Single Tube Strategy Enabling Isothermal Analysis of MicroRNA at Sub-Attomole Level. *Biosens. Bioelectron.* **2016**, 80, 378–384.

49. Zhang, D. Y.; Hariadi, R. F.; Choi, H. M. T.; Winfree, E. Integrating DNA Strand-Displacement Circuitry with DNA Tile Self-Assembly. *Nat. Commun.* 2013, 4, **1965**.

50. Ma, C.; Zhang, M.; Chen, S.; Liang, C.; Shi, C. Rapid and Enzyme-Free Nucleic Acid Detection Based on Exponential Hairpin Assembly in Complex Biological Fluids. *Analyst* **2016**, 141, 2883–2886.

51. Hall, B.; Cater, S.; Levy, M.; Ellington, A. D. Kinetic Optimization of a Protein-Responsive Aptamer Beacon. *Biotech. Bioeng.* **2009**, 103, 1049–1059.

52. Meagher, R. J.; Won, J.-i.; McCormick, L. C.; Nedelcu, S.; Bertrand, M. M.; Bertram, J. L.; Drouin, G.; Barron, A. E.; Slater, G. W. End-Labeled Free-Solution Electrophoresis of DNA. *Electrophoresis* **2005**, 331–350.

53. Nkodo, A. E.; Garnier, J. M.; Tinland, B.; Ren, H.; Desruisseaux, C.; McCormick, L. C.; Drouin, G.; Slater, G. W. Diffusion Coefficient of DNA Molecules During Free Solution Electrophoresis. *Electrophoresis* **2001**, 22, 2424–2432.

54. Frank, S.; Winkler, R. G. Polyelectrolyte Electrophoresis: Field Effects and Hydrodynamic Interactions. *EPL* **2008**, 83, 38004.

55. Stellwagen, N. C.; Gelfi, C.; Righetti, P. G. The Free Solution Mobility of DNA. *Biopolymers* **1997**, 42, 687–703.

56. Nedelcu, S.; Slater, G. W. Branched Polymeric Labels Used as Drag-Tags in Free-Solution Electrophoresis of ssDNA. *Electrophoresis* **2005**, 26, 4003–4015.

57. Sampson, H. A. Utility of food-specific IgE concentrations in predicting symptomatic food allergy. *J. Allergy Clin. Immunol.* **2001**, 107, 891–896.

58. Grimbacher, B.; Holland, S. M.; Puck, J. M. Hyper-IgE syndromes. *Immunol. Rev.* **2005**, 203, 244–250.

59. Ogawa, M.; Kochwa, S.; Smith, C.; Ishizaka, K.; McIntyre, O. R. Clinical Aspects of IgE Myeloma. *N. Engl. J. Med.* **1969**, 281, 1217–1220.

60. Wiegand, T. W.; Williams, P. B.; Dreskin, S. C.; Jouvin, M. H.; Kinet, J. P.; Tasset, D. High-Affinity Oligonucleotide Ligands to Human IgE Inhibit Binding to Fc Epsilon Receptor I. *J. Immunol.* **1996**, 157, 221–30.

61. Turgeon, R. T.; Fonslow, B. R.; Jing, M.; Bowser, M. T. Measuring Aptamer Equilibria Using Gradient Micro Free Flow Electrophoresis. *Anal. Chem.* **2010**, 82, 3636–3641.

1
2
3
4
5
6
7
8
9
10
11
12
13
14
15
16
17
18
19
20
21
22
23
24
25
26
27
28
29
30
31
32
33
34
35
36
37
38
39
40
41
42
43
44
45
46
47
48
49
50
51
52
53
54
55
56
57
58
59
60

For TOC only

